

" $A_2$ " MESON PRODUCTION FROM  $K^-n$  INTERACTIONS AT 3.9 GeV/c \*

David J. Crennell, Uri Karshon,† Kwan Wu Lai, John S. O'Neill, and J. Michael Scarr  
Physics Department, Brookhaven National Laboratory, Upton, New York 11973

(Received 23 April 1969)

We report the observation of one narrow  $\rho^0\pi^-$  resonance in the  $A_2(1300)$  mass region with a width of 40 MeV or less from the reaction  $K^-n \rightarrow \Lambda\rho^0\pi^-$ . A spin-and-parity analysis of this narrow enhancement favors  $J^{PC}=1^{-+}$ . Branching ratios for other decay modes are also given.

The recent discovery of the splitting of the  $A_2(1300)$  meson<sup>1</sup> produced in  $\pi p$  interactions requires a careful re-examination of spin and parity assignments in this region. Since there are two distinct peaks in this mass region, which have been named the  $A_2^H(1315)$  and  $A_2^L(1270)$ ,<sup>2</sup> it is extremely important to study the mass and width as well as angular correlations for each possible decay mode independently before associating it with either  $A_2^H$  or  $A_2^L$ .

In this Letter we report a study of the  $\rho\pi$ ,  $\eta(550)\pi$ , and  $K\bar{K}$  decay modes of the " $A_2$ " as observed in the reaction  $K^-n \rightarrow \Lambda$ " $A_2$ " at 3.9 GeV/c. In the  $\rho^0\pi^-$  channel a single narrow peak is seen in the " $A_2$ " mass region with a width of 40 MeV or less. This contrasts to previous results on the  $\rho\pi$  mode as a single peak with a width of  $90 \pm 10$  MeV obtained in  $\pi N$  interactions.<sup>3</sup> A spin-and-parity analysis of the events in this narrow  $\rho^0\pi^-$  ( $I^G=1^-$ ) resonance favors  $J^{PC}=1^{-+}$  as the simplest assignment.

Approximately 200 000 pictures obtained from the Brookhaven National Laboratory 80-in. liquid-deuterium bubble chamber exposed to 3.9-GeV/c  $K^-$  mesons were analyzed.<sup>4</sup> 2740 events fitted the final state  $\Lambda\pi^-\pi^+\pi^-$ , 173 events fitted  $\Lambda\eta(550)\pi^- \rightarrow \Lambda\pi^-\pi^+\pi^-$  ( $\pi^0$  or  $\gamma$ ), and 42 events fitted  $\Lambda K^-K_1^0$ . Visible  $\Lambda$  decays were required in all cases and, in addition, a visible  $K^0$  decay in  $\Lambda K^-K_1^0$ .

In studying the  $\rho^0\pi^-$  system produced in the  $\Lambda\rho^0\pi^-$  final state it is desirable to remove that background which is due to the final states  $\Sigma(1385)^\pm\pi^\mp\pi^-$  and  $\Sigma(1385)^-\rho^0$ . Strong  $\Sigma(1385)^\pm \rightarrow \Lambda\pi^\pm$  is seen, with approximately 50% of the events having at least one  $\Lambda\pi^\pm$  effective mass in the region 1340-1420 MeV. Figure 1(a) shows the  $\pi^-\pi^+$  mass distribution for those combinations in which either pion gives a  $\Lambda\pi$  effective mass in the  $\Sigma(1385)$  mass region. There is no evidence of  $\rho^0$  and  $\Sigma(1385)^\pm$  sharing the same pion. In contrast, Fig. 1(b) shows strong  $\rho^0$  production for those events with no  $\Lambda\pi^\pm$  effective mass in the  $\Sigma(1385)^\pm$  region. Therefore, in the subsequent analysis of the  $\rho^0\pi^-$  events the

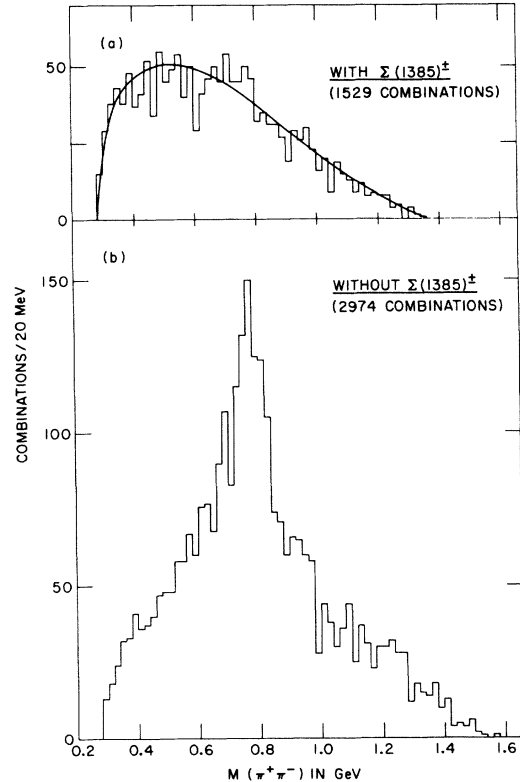


FIG. 1. The  $\pi^+\pi^-$  mass distributions with  $\Lambda\pi$  mass selections (as shown) from the  $\Lambda\pi^+\pi^-\pi^-$  final state.

$\Sigma(1385)^\pm\pi^\mp\pi^-$  and  $\Sigma(1385)^-\rho^0$  backgrounds are suppressed by rejection of all events with a  $\Lambda\pi^\pm$  effective mass in the  $\Sigma(1385)$  region.

The three-pion mass distribution for the 746 events with at least one  $\pi^+\pi^-$  mass combination in the  $\rho^0$  mass region (650-880 MeV) is shown in Fig. 2(a). A broad enhancement at  $\sim 1.1$  GeV corresponding to the  $A_1$  mass and a sharp peak in the  $A_2$  mass region are evident. We note that the  $\rho^0\pi^-$  background in the low  $\rho^0\pi^-$  mass region is considerably less in this reaction ( $K^-n \rightarrow \Lambda\rho^0\pi^-$ ) than in the comparable  $\pi p$  interactions ( $\pi^-p \rightarrow p\rho^0\pi^-$ ), where the usual Deck mechanism prevails. Therefore, our data give strong support to the resonance interpretation of the  $A_1$  enhancement at a mass  $\sim 1100 \pm 10$  and width  $90 \pm 30$  MeV.

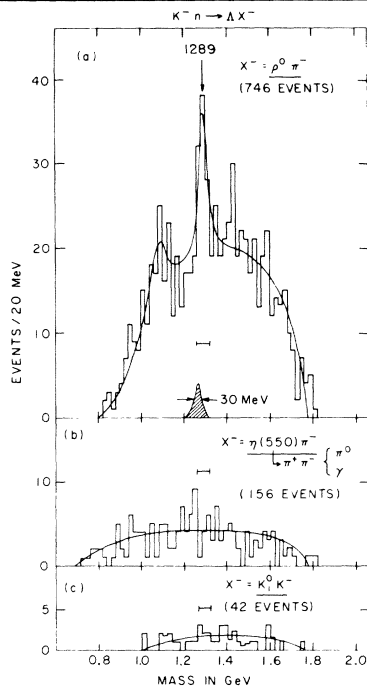


FIG. 2. (a)  $\rho^0\pi^-$  mass distribution with events in  $\Sigma(1385)^\pm$  region removed. A best fit to the data for two resonances and phase space is shown in the solid curve. Mass resolution in the " $A_2$ " region is shown in the hatched area. (b)  $\eta(550)\pi^-$  mass distribution with events in the  $\Sigma(1385)^-$  region removed. The curve shows phase space. (c)  $K^-K_1^0$  mass distribution. The curve again shows phase space.

The properties of the narrow " $A_2$ " resonance are examined below:

(1) **Mass.**—From a fit to the  $\rho^0\pi^-$  effective-mass distribution, calculated from measured variables, the " $A_2$ " mass is found to be  $1289 \pm 10$  MeV. For comparison the measured  $K_1^0$  mass gave a value of 497.0 MeV in good agreement with the accepted value of 497.8 MeV.<sup>5</sup> Unlike this procedure, the missing-mass experiments<sup>1,2</sup> for the reaction  $\pi^-p \rightarrow p\pi^-$ , which find mass values  $A_2^H(1315 \pm 4)$  and  $A_2^L(1269 \pm 5)$ , depend directly on an absolute measurement of beam momentum.<sup>6</sup> Thus the mass values must be compared with caution because of possible systematic differences.

(2) **Width.**—The apparent width of this sharp peak from our fitting procedures is  $50 \pm 10$  MeV. Unfolding the mass resolution of 30 MeV ( $\Delta M = \pm 15$  MeV) yields a true width of 40 MeV or less with 90% confidence. This value is substantially less than those deduced from  $\pi N$  interactions<sup>3</sup> ( $90 \pm 10$  MeV) from a one-peak assumption of the " $A_2$ ," but is compatible with the widths of either  $A_2^H$  or  $A_2^L$ , namely  $25 \pm 10$  MeV.

(3) **Isospin, charge conjugation, and G parity.**

—The production of this " $A_2$ " in the reaction  $K^-n \rightarrow \Lambda "A_2"$  requires the assignment  $I=1$ , and assuming a strong decay to  $\rho^0\pi^-$  makes  $G=-1$  and the charge conjugation  $C_\eta = +1$  for the neutral member of this isotriplet resonance.

(4) **Relative branching ratios.**—We have examined the final states  $\Lambda\eta(550)\pi^-$  with  $\Sigma(1385)^-$  events removed and  $\Lambda K^-K_1^0$  for the " $A_2$ " decay modes  $\eta(550)\pi^-$  with charged  $\eta$  decay and  $K^-K_1^0$  with visible  $K_1^0$ . The mass distributions are shown in Figs. 2(b) and 2(c). The upper limits for  $\eta(550)\pi$  and  $K\bar{K}$  with respect to  $\rho\pi$  are 33 and 23%, respectively, at the 95% confidence level.

(5) **Spin and parity.** (a) **Three-pion Dalitz-plot analysis.**—Since the dominant decay of the " $A_2$ " is  $\rho\pi$ , the analysis is confined to examination of events in the  $\rho$  bands of the three-pion ( $\pi^+\pi_a^-\pi_b^-$ ) Dalitz plot using Zemach's method.<sup>7</sup> For each  $\rho^0$  ( $\pi_a^-\pi^+$ ) band the alternative mass-squared distribution  $M^2(\pi_b^-\pi^+)$  is plotted, the events in the  $\rho^0$  overlap region being plotted twice. Figures 3(e)-3(g) show these distributions for three regions of  $\rho^0\pi^-$  mass, one covering the " $A_2$ " mass region (1260-1320 MeV) and the other two for control regions below (1140-1260 MeV) and above (1320-1440 MeV) the " $A_2$ " region. The fit to the distribution in the " $A_2$ " region includes the effect of an incoherent background which is determined as follows<sup>8</sup>: The fraction of signal to background  $B$  in the " $A_2$ " region  $B$  is determined to be  $0.55 \pm 0.05$  from a fit to the  $\rho\pi$  mass spectrum of Fig. 2(a) using a Breit-Wigner form for the  $A_1$  and " $A_2$ " peaks together with an incoherent phase-space background. This background is then taken to be of two parts: a three-pion phase space uniformly distributed over the Dalitz plot and a  $\rho^0\pi^-$  background which we have assumed to behave as a  $1^+$  ( $s$ -wave) state. The ratio  $X$  of three-pion background to all background has been estimated by examining the  $\pi^+\pi^-$  mass distributions in the " $A_2$ " region and the two control regions [from the total three-pion spectrum with  $\Sigma(1385)^\pm$  events removed] giving  $X = 0.3 \pm 0.2$ . The curves in Figs. 3(e) and 3(g) show the expected background distribution for  $X=0.3$  and indicate that our assumptions about the background are able to describe the control regions. We have considered only those possible spin and parity assignments for the " $A_2$ " which have  $J \leq 2$  and the lowest possible orbital angular momentum states for each value of  $J^P$ , namely,  $0^-$  ( $p$  wave),  $1^+$  ( $s$  wave),  $2^-$  ( $p$  wave),  $1^-$  ( $p$  wave), and  $2^+$  ( $d$  wave). For each spin-and-parity hypothesis the " $A_2$ " region has

been fitted by incoherent addition of signal, three-pion, and  $\rho\pi$  backgrounds for a wide range of  $X$  and  $B$ . The resulting  $\chi^2$  is then calculated allowing for the double counting in the  $\rho^0$  overlap region. The  $0^-$  ( $p$ -wave) assignment is clearly ruled out. The  $1^+$  ( $s$ -wave) and  $2^-$  ( $p$ -wave) assignments give similar distributions and also give similar  $\chi^2$  as for the case of the  $2^+$  assignment.  $\chi^2$  curves for  $J^P = 1^-$  (solid line) and  $J^P = 2^+$  (dashed line) are shown as a function of  $B$  for three values of  $X$  in Figs. 3(a)-3(c) and in Fig. 3(d) for  $B = 0.5$  as a function of  $X$ . Using the estimated values of  $B$  and  $X$ , the  $\chi^2$  probabilities for the hypotheses  $1^-$  and  $2^+$  are, respectively, 25 and 2%. The corresponding curves for the  $M^2(\pi^+\pi^-)$  spectra are shown in Fig. 3(f). We note that the values of  $\chi^2$  obtained are insensitive to the value of  $X$ . The better fit to  $1^-$  is due largely to the absence of a peak at  $M^2(\pi^+\pi^-) \sim 0.6 \text{ GeV}^2$  expected from the constructive interference in the  $\rho^0$  overlap region for the  $2^+$  assignment.

(b) The  $(\rho^0\pi^-)$  decay angular distributions. — We now examine the orientation of the normal to the three-pion decay plane,<sup>9</sup> an angular distribution independent of the previously considered  $M^2(\pi^+\pi^-)$  distribution. Figures 3(h) and 3(i) show the polar ( $\cos\Theta$ ) and the Treiman-Yang ( $\Phi$ ) distributions for the “ $A_2$ ” region. The  $\cos\Theta$  distribution for the “ $A_2$ ” shows marked peaking at  $\cos\Theta = \pm 1$  with only a 3% probability of consistency with being flat like the two control regions (not shown). The Treiman-Yang distribution is flat in all three regions. The  $\cos\Theta$  distributions for the events in the “ $A_2$ ” region have been fitted to  $J^P = 1^-$  and  $2^+$ . Assuming an incoherent isotropic background with  $B = 0.55$  the following results are obtained: (i) For  $J^P = 1^-$ ,  $\rho_{00} = 0.87 \pm 0.1$  with  $\chi^2$  probability of 40%, and (ii) for  $J^P = 2^+$ ,  $\rho_{11} = 0.38 \pm 0.11$  ( $\rho_{22}$  constrained = 0) with  $\chi^2$  probability 6%. However, if one assumes strong interference between a  $2^+$  state and an  $s$ -wave background, essentially allowing  $\rho_{22}$  to be negative, the  $2^+$  fit can be made as good as  $1^-$ .

The above two independent analyses both favor  $J^P = 1^-$  over  $2^+$ . This assignment  $J^PC = 1^{-+}$  precludes a  $K\bar{K}$  decay mode and is consistent with our observation [Fig. 2(c)]. However, the value  $\rho_{00} = 0.87$  obtained in the  $\rho^0\pi^-$  decay analysis, if interpreted with a simple one-particle-exchange model, suggests dominantly spin-0 exchange. The only candidate, the  $K^0$ , is however excluded by the above argument. However, the “ $A_2$ ” production angular distribution, shown in Fig. 3(j), does not indicate strong peripheral production

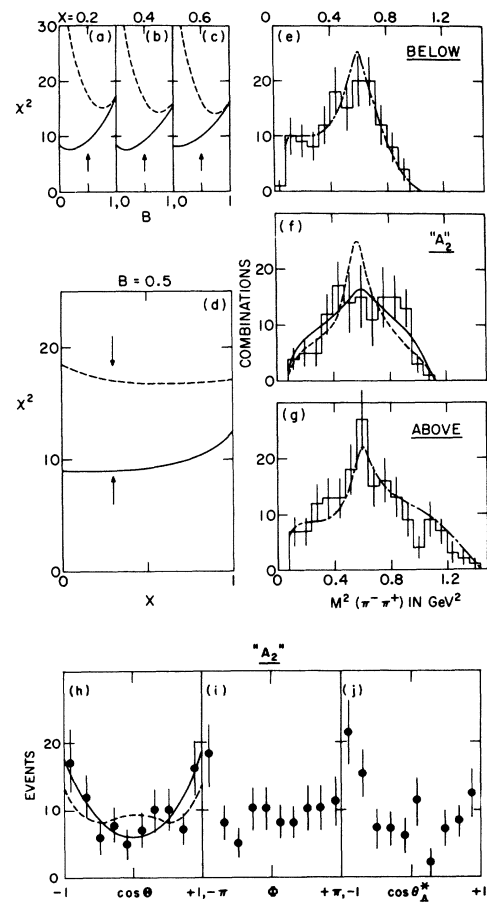


FIG. 3. (a)-(g) Dalitz plot fits described in text. (a)-(d) Variations of  $\chi^2$  (six degrees of freedom), with varying fraction of background ( $B$ ) and the ratio ( $X$ ) of  $3\pi/\rho\pi$  in the background, for  $J^P = 1^-$  (solid line) and  $J^P = 2^+$  (dashed line) fits to the “ $A_2$ ” region. The arrows indicate the best values of  $B$  and  $X$ . (e)-(g)  $\pi^+\pi^-$  mass-squared distributions for events in the  $\rho$  band for three  $\rho\pi$  mass regions. Curves in (e) and (g) show the expected background distributions. The expected distributions for  $J^P = 1^-$  (solid line) and  $J^P = 2^+$  (dashed line) in the “ $A_2$ ” region are shown in (f). (h) and (i) Angular distribution of the three-pion decay plane for the “ $A_2$ ” region with the polar angle  $\cos\Theta$  and the Treiman-Yang angle  $\Phi$ . (j) “ $A_2$ ” production angular distribution.

and suggests that single-particle exchange may not be the dominant production mechanism.

In conclusion, our investigation of the “ $A_2$ ” meson produced in the  $K^-n$  interaction at 3.9 GeV/c can be summarized as follows:

(1) We have observed a narrow  $\rho^0\pi^-$  resonance in the “ $A_2$ ” mass region with a width less than 40 MeV. This value is incompatible with that from a previous single-peak assumption of the “ $A_2$ ” meson, namely,  $90 \pm 10 \text{ MeV}$ . This observation suggests that we have observed one and

not both peaks of the "A<sub>2</sub>." In addition the mass of this narrow resonance (1289 ± 10 MeV) is centered below 1300 MeV.

(2) Two independent spin and parity analyses of this  $\rho^0\pi^-$  resonance favor the assignment  $J^{PC} = 1^{-+}$  (25%, 40%) over  $J^{PC} = 2^{++}$  (2%, 6%). This is again different from previous investigations of the "A<sub>2</sub>" -  $\rho\pi$  either as single or double peaks.

If this narrow  $\rho^0\pi^-$  resonance is indeed a  $J^{PC} = 1^{-+}$  particle, then it will be difficult to accommodate it in the simple ( $\bar{q}q$ ) model for particle classifications where  $P=C$  for all natural-parity states, such as the  $\rho$  meson ( $J^{PC} = 1^{--}$ ). It may be necessary to invoke new models for particle classifications such as the four-dimensional ( $q\bar{q}$ ) harmonic-oscillator model, or the existence of daughter trajectories in the Chew-Frautschi plot, or both.<sup>10</sup>

We wish to acknowledge the support and encouragement of Dr. Ralph P. Shutt. It is also a pleasure to thank the Brookhaven alternating-gradient synchrotron bubble-chamber and data-reduction staffs for their assistance.

\*Work performed under the auspices of the U. S. Atomic Energy Commission.

†On leave of absence from the Weizmann Institute of Science, Rehovoth, Israel.

<sup>1</sup>H. Benz *et al.*, Phys. Letters **28B**, 233 (1968), and references therein.

<sup>2</sup>D. J. Crennell, U. Karshon, K. W. Lai, J. M. Scarr, and I. O. Skillicorn, Phys. Rev. Letters **20**, 1318 (1968).

<sup>3</sup>See a compilation by B. French, in Proceedings of the Fourteenth International Conference on High-Energy Physics, Vienna, Austria, 1968 (CERN Scientific Information Service, Geneva, Switzerland, 1968), p. 107.

<sup>4</sup>See D. J. Crennell *et al.*, Phys. Rev. Letters **21**, 648 (1968); Benz *et al.*, Ref. 1; Crennell, Karshon, Lai, Scarr, and Skillicorn, Ref. 2.

<sup>5</sup>See a compilation by N. Barash-Schmidt *et al.*, Rev. Mod. Phys. **41**, 109 (1969).

<sup>6</sup>W. Kienzle, in Proceedings of an Informal Meeting on Experimental Meson Spectroscopy, Philadelphia, Pennsylvania, 1968 (W. A. Benjamin, Inc., New York, 1968), p. 265.

<sup>7</sup>We have used the program of R. Diebold [CERN Report No. CERN/TC/PROG. 64-25 (unpublished)] to calculate the Dalitz-plot distributions in the  $\rho^0$  bands. The program uses the formalism of C. Zemach, Phys. Rev. **133**, B1201 (1964).

<sup>8</sup>A similar approach has been used by S. U. Chung *et al.* [Phys. Rev. Letters **18**, 100 (1967)] and A. W. Key *et al.* [Phys. Rev. **166**, 1430 (1968)].

<sup>9</sup>The normal is defined in the three-pion rest frame by  $n = \pi_a^- \times \pi_b^-$ , where the lower momentum  $\pi^-$  has been taken first. The axes are defined in this frame with the  $z$  direction in the direction of the incident  $K^-$  and the  $y$  direction normal to the  $A_2$  production plane.  $\Theta$  and  $\Phi$  are then the polar and azimuthal angles. Maximum likelihood fits were made to the combined  $\Theta$  and  $\Phi$  distribution. Possible distributions are given by S. M. Berman and M. Jacob, Phys. Rev. **139**, B1023 (1965).

<sup>10</sup>For a review of recent theoretical development, see H. Harari, in Proceedings of the Fourteenth International Conference on High-Energy Physics, Vienna, Austria, 1968 (CERN Scientific Information Service, Geneva, Switzerland, 1968), p. 195.

## BROKEN-DUALITY MODEL FOR THE REACTION $pp \rightarrow \pi^+d$ \*

V. Barger and C. Michael

Department of Physics, University of Wisconsin, Madison, Wisconsin 53706

(Received 28 April 1969)

A model based on a broken ( $N_\alpha, N_\gamma$ ) exchange degeneracy is proposed to explain the structureless data for the  $pp \rightarrow \pi^+d$  differential cross section. An effective Regge trajectory is determined which agrees with our prediction. Quantitative fits to the data are presented and physical aspects of the broken degeneracy are discussed.

The appropriate theoretical description of the accumulated data on the reaction  $pp \rightarrow \pi^+d$  has remained as an unsolved problem during this period in which Regge-exchange models have accounted for a substantial fraction of two-body scattering reactions. The only systematic approach to the  $pp \rightarrow \pi^+d$  data<sup>1-4</sup> proposed thus far is the empirical formula  $\exp(-\alpha p_\perp)$ , which unfortunately has no sound theoretical basis.

In terms of exchange models, the  $u$  and  $t$  channels for  $pp \rightarrow \pi^+d$  are  $B=1$  and  $I=\frac{1}{2}$ , and the nu-

cleon is an obvious candidate for exchange. In fact, from the nucleon Regge pole we expect the integrated cross section to have an energy dependence

$$\sigma \sim s^{-3},$$

which is crudely compatible with the data. However, for nucleon exchange conventional Regge theory also predicts a differential-cross-section zero<sup>5</sup> at  $u \simeq -0.15$  (GeV/c)<sup>2</sup> where  $\alpha_N(u) = -\frac{1}{2}$ . This strongly contradicts the data which show